NEW TECHNIQUE FOR CALCULATING ICE DEPTHS ON MARS AT THEMIS RESOLUTION. J. Buz[1], C. S. Edwards[1], S. Piqueux[2], [1]Northern Arizona University Department of Physics and Astronomy, Flagstaff, AZ 86011, [2]Jet Propulsion Laboratory, California Institute of Technology. Contact: jennifer.buz@nau.edu

Introduction: The high latitude regions of Mars have shallow subsurface ice as inferred by hydrogen abundance measurements with the Gamma Ray Spectrometer (GRS) instrument [1–3] and observed by the Phoenix Mars Lander [4–6]. Determining the depth to any ice-rich layer has significance for future mission planning and in-situ resource utilization. Although water ice depth is shown to generally increase with latitude, local features such as slope, albedo, and thermal inertia of the ground cover are major influences [7–9]. Using repeat observations taken by the Thermal Emission Imaging System (THEMIS) at different seasons enables high resolution calculations of the thermophysical properties of the surface and the effect of subsurface ice [e.g., 9]. While the information gained from utilizing the high resolution THEMIS dataset is critical, the increase in data volume presents unique problems to the thermophysical modeling. We present two modifications to previously employed ice depth calculation techniques which we propose simultaneously improve the measurement accuracy and efficiency.

Methods: We use the KRC numerical thermal model in conjunction with a DaVinci Interface (krc.mars.asu.edu) to compute thermal inertia and depth to ice [10]. Similar to Bandfield and Feldman [11], we assume a two-layered geometry of dry soil on top of a water rich layer. We find two overlapping THEMIS night-time images which were taken during significantly different season (i.e. > 100° solar longitude (L_s)). As demonstrated in Bandfield [9], there is a crossover L_s during which the surface temperature is unaffected by the depth to subsurface ice, referred to as L_s* (Figure 1: this will be a modification of Bandfield 2007 Figure 1 where the crossover point is labeled L_s*). We select one of our THEMIS images to lie close to L_s* which has been previously modeled for the entire Mars surface by Piqueux [12] and use this image to calculate the thermal inertia of the surface. Our model inputs for this calculation include latitude, local time, season, slope, albedo, dust opacity (modeled for a given Mars year and latitude), elevation, and azimuth. To invoke the "one-point" mode of KRC [10] we also input the THEMIS band 9 (12.57 μm) brightness temperature and an initial guess of the thermal inertia which comes from a global thermal inertia map generated using lower resolution Thermal Emission Spectrometer (TES) data. We then create a look-up table for various surface temperature v. ice depth pairs using the standard KRC algorithm with the thermal inertia calculated in the previous step as input and observation parameters which match our second THEMIS image from earlier in the Mars year (Figure 2: This will be a plot of a set of depth v temperatures). We use the band 9 brightness temperature from the second image and interpolate between the values of the look-up table to estimate the depth to ice at each point.

Modifications from previous techniques: The use of THEMIS for surface temperature, thermal inertia, and depth to ice calculations enables the highest-resolution maps to be produced. This is a benefit over the lower resolution TES temperatures used in previous studies [e.g., 11]. Furthermore, selecting images acquired within L_s* allowed for independent calculation of thermal inertia and depth to ice, these parameters have been calculated together in previous works [e.g., 9]. Lastly, the use of KRC one-point mode dramatically reduces the computational time for thermal inertia derivation. In addition to these modeling modifications, we have parallelized our computations by taking advantage of the fact that each pixel can be calculated independently of the rest. The large data volume can therefore be segmented to the limitations of the computational system. For example, by conducting calculations on one row of the THEMIS image at a time we are able to reduce the computation time by a factor greater than 1000. Through this parallelization, maps of buried ice over large portions of Mars can be easily generated.

Future Work: We will target regions where past maps of ice depth using thermophysical modeling are discrepant with neutron detections. In particular, we will investigate the effect of slope on the depth to buried ice, since slope can be a proxy for a change in latitude.

Acknowledgements: Part of this work was performed at the Jet Propulsion Laboratory, California Institute of Technology, under a contract with NASA. Government support acknowledged.

References: [1] Feldman W. C. et al. (2004) *J. Geophys. Res. Planets* **109**, DOI 10.1029/2003JE002160. [2] Boynton W. V et al. (2002) *Science (80-.).* **297**, 81 LP-85. [3] Mitrofanov I. G. et al. (2004) *Sol. Syst. Res.* **38**, 253–257. [4] Mellon M. T. et al. (2009) *J. Geophys. Res. Planets* **114**, DOI 10.1029/2009JE003417. [5] Smith P. H. et al. (2009) *Science (80-.).* **325**, 58 LP-61. [6] Arvidson R. E. et al. (2009) *J. Geophys. Res.* **114**, DOI Artn E00e02

10.1029/2009je003408. [7] Sizemore H. G. and Mellon M. T. (2006) *Icarus* **185**, 358–369. [8] Aharonson O. and Schorghofer N. (2006) *J. Geophys. Res. Planets* **111**, DOI 10.1029/2005JE002636. [9] Bandfield J. L. (2007) *Nature* **447**, 64. [10] Kieffer H. H. (2013) *J. Geophys. Res. Planets* **118**, 451–470. [11] Bandfield J. L. and Feldman W. C. (2008) *J. Geophys. Res. Planets* **113**, DOI 10.1029/2007JE003007. [12] Piqueux S. et al. (2018) *5th European Conference on Permafrost*, pp. 733–734.

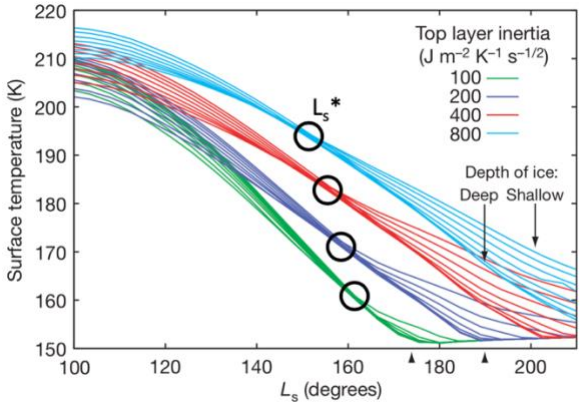

Figure 1
Modification of Figure 1 from Bandfield [9] indicating crossover point, L_s*, where depth to ice is not affected by top layer thermal inertia. Thermal inertia of the surface is calculated from THEMIS data acquired during tis L_s*.

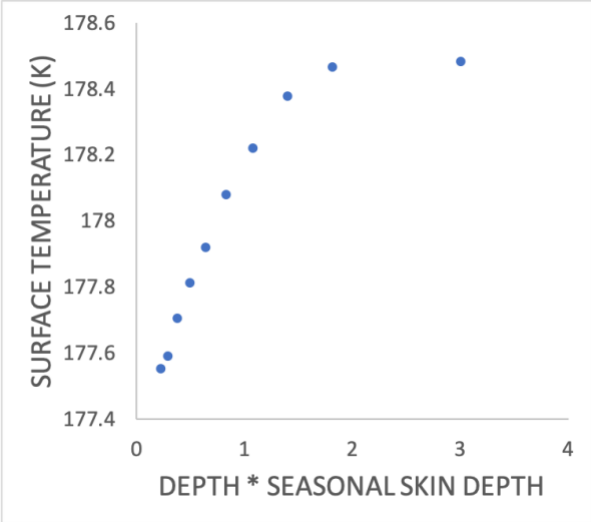

Figure 2
Effect of depth-to-ice rich layer on surface temperature. This relationship is calculated for each pixel using the slope, albedo, modeled atmospheric opacity, elevation, azimuth, season, local time, and previously calculated thermal inertia. A thermal inertia of 2261 is used for the second layer, following Bandfield [11].